Available online at www.sciencedirect.com
ScienceDirect
International Journal of Solids and Structures 44 (2007) 2209–2224
INTERNATIONAL JOURNAL OF SOLIDS and STRUCTURES
www.elsevier.com/locate/ijsolstr

Non-linear cancellation of the parametric resonance in elastic beams: Theory and experiment

Walter Lacarbonara [a,*], Hiroshi Yabuno [b], Keiichi Hayashi [b]

[a] *Dipartimento di Ingegneria Strutturale e Geotecnica, University of Rome La Sapienza, via Eudossiana 18, Rome 00184, Italy*
[b] *Graduate School of Systems and Information Engineering, University of Tsukuba, Tsukuba-City 305-8573, Japan*

Received 20 January 2006; received in revised form 10 May 2006
Available online 13 July 2006

Abstract

A non-linear control strategy is applied to a simply supported uniform elastic beam subjected to an axial end force at the principal-parametric resonance frequency of the first skew-symmetric mode. The control input consists of the bending couples applied by two pairs of piezoceramic actuators attached onto both sides of the beam surfaces and symmetrically with respect to the midspan, driven by the same voltage, thus resulting into symmetric control forces. This control architecture has zero control authority, in a linear sense, onto skew-symmetric vibrations. The non-linear transfer of energy from symmetric motions to skew-symmetric modes, due to non-linear inertia and curvature effects, provides the key physical mechanism for channelling suitable control power from the actuators into the linearly uncontrollable mode. The reduced dynamics of the system, constructed with the method of multiple scales directly applied to the governing PDE's and boundary conditions, suggest effective forms of the control law as a two-frequency input in sub-combination resonance with the parametrically driven mode. The performances of different control laws are investigated. The relative phase and frequency relationships are designed so as to render the control action the most effective. The control schemes generate non-linear controller forces which increase the threshold for the activation of the parametric resonance thus resulting into its annihilation. The theoretical predictions are compared with experimentally obtained results.

Keywords: Resonance cancellation; Non-linear control; Parametric resonance; Sub-combination resonance; Direct method of multiple scales

1. Introduction

The task of copying with resonant disturbances such as parametric excitations has been tackled in many different ways from direct active disturbance rejection via classical control theory methods to the use of passive vibration absorbers.

A number of works has addressed both theoretically and experimentally the problem of controlling transverse oscillations by parametric-type control actions in distributed-parameter systems (Fujino et al., 1993) or

* Corresponding author. Tel.: +39 06 44585293; fax: +39 06 4884852.
E-mail address: walter.lacarbonara@uniroma1.it (W. Lacarbonara).

0020-7683/$ - see front matter © 2006 Elsevier Ltd. All rights reserved.
doi:10.1016/j.ijsolstr.2006.07.004

by coupling autoparametrically the system to an electronic circuit (Oueini et al., 1998) or to a passive absorber (Yabuno et al., 2004a). In particular, Yabuno and co-workers showed that a parametric resonance in a cantilever beam can be suppressed by attaching a pendulum absorber to the beam tip.

The active suppression of parametric resonances has also attracted numerous researchers. Among others, Oueini and Nayfeh (1999) devised a cubic feedback law to suppress the vibrations of the first mode of a cantilever beam when subjected to a principal parametric resonance. Maccari (2001) investigated the parametric resonance of a van der Pol oscillator under state feedback control with a time delay and found appropriate feedback gains and time delay to prevent quasi-periodic motions and to reduce the amplitude peak of the parametric resonance. Ji and Leung (2002) used a linear time-delayed feedback control to shift the occurrence of pitchfork bifurcations and to eliminate saddle-node bifurcations, which may arise in the non-linear response of a parametrically excited Duffing system under its principal parametric resonance. They showed that, with appropriate feedback gains, the stable region of the trivial solutions can be broadened. Watanabe et al. (2003) proposed a robust damping control in a power electric system capable of maintaining stability also in the presence of an auto-parametric resonance. Because they used a model with a certain structure and uncertain parameters, they designed a robust controller via μ-synthesis, alternative to other existing methods based on H-infinity control. All of these investigations share the common feature of proposing non-linear laws to control parametric resonances; however, the problem of collocation of the control action is not specifically addressed.

Inspired by previous studies, a general methodology was proposed (Lacarbonara et al., 2002) to design, via asymptotic approaches, non-linear open-loop resonance-cancellation schemes. It was shown that a direct perturbation expansion of the system dynamics facilitates understanding of the non-linear mechanisms by which the actuator inputs may be used to suppress the resonant effects of the excitation. Depending on the specific system, various non-linear mechanisms for generating effective actuator actions may be exploited. Moreover, when excitations and actuations are non-collocated (e.g., when the actuation has zero projection, in a linear sense, on the dynamics to be controlled), classical linear control techniques break down. On the contrary, due to the inherent non-linear internal forces, the controller action, although non-collocated, may be intelligently designed to have sufficient authority to cancel or significantly mitigate the resonances.

To show the feasibility of the open-loop resonance-cancellation methodology, a control strategy was devised (Lacarbonara et al., 2002) for a shallow arch subject to a harmonic longitudinal end displacement that is parametrically resonant with the first skew-symmetric mode and the control input is a transverse force at the midspan. The effective mechanism was shown to be a sub-harmonic resonance of order one-half. In a previous work (Soper et al., 2001), similar concepts were employed to address non-collocated disturbances via non-linear actuator action in a pendulum-type crane architecture. Moreover, to show the possibility of enhancing the non-linear control authority with more general disturbances, Lacarbonara and Yabuno (2004) proposed a closed-loop non-linear scheme to control the first skew-symmetric mode of a hinged–hinged initially curved beam driven to resonance by an external primary-resonance disturbance.

Recently, the method of parametric resonance cancellation (Lacarbonara et al., 2002) has been theoretically and experimentally demonstrated in a magnetically levitated body (Yabuno et al., 2004b). Therein, the principal parametric resonance of the levitated body has been stabilized using an actively driven pendulum-type vibration device.

The present work investigates an open-loop scheme tailored to cancel the parametric resonance of the first skew-symmetric mode of a beam which is hinged at one end and acted upon by a time-varying load on the other end, a roller support with a lumped mass. The symmetric control action – bending moments imparted by two pairs of symmetrically attached piezoceramic actuators – is non-collocated as it is orthogonal, in a linear sense, to the externally excited mode. The control input is designed so as to be capable of suppressing the resonant part of the beam flexural vibrations with feasible control efforts. Proving that a non-linear controller with a symmetric input can reduce also skew-symmetric vibrations entails that the control authority is expanded in comparison with the linear theory by exploiting the structural non-linearities. The same controller, designed primarily to reduce symmetric oscillations, may be used to reduce skew-symmetric vibrations which, under some excitation conditions (e.g., at the so-called crossovers), can be excited simultaneously with symmetric vibrations. Because the fact that a symmetric input has control authority over symmetric vibrations is trivial, in the present study, the effectiveness of the symmetric non-linear input in reducing skew-symmetric

vibrations of an elastic beam is theoretically investigated and experimentally validated. The designed control law is a two-frequency input in sub-combination resonance with the frequency of the parametrically excited mode.

The paper is organized as follows. In Section 2, the geometrically exact equations of motion of the beam including the piezoceramic actuators are presented. In Section 3, the derivation of the open-loop control strategy via a direct perturbation treatment of the governing equations of motion, including the controllers, is discussed. In Section 4, the features of the theoretically and experimentally obtained uncontrolled and controlled responses are documented and discussed. In Section 5, the concluding remarks are presented.

2. Equations of motion

In this section, following (Lacarbonara and Yabuno, 2006), the mechanical formulation to describe overall planar motions of slender beams, with the addition of the controllers, is summarized. The beam is straight in its reference configuration $\mathscr{C}_0$ (Fig. 1 top); it is assumed sufficiently slender with a compact cross-section and is made of a hyperelastic and homogeneous material. It is further assumed that, due to its slenderness, the beam is unshearable and, due to the axially unrestrained nature of the motions, it is inextensible.

A Lagrangian description of the motion is adopted. Denoting with $\mathbf{e}_i$ $(i = 1,2,3)$ the orthonormal unit vectors of a fixed inertial reference frame in $\mathbb{E}^3$ Euclidean space such that $\mathbf{e}_1$ is parallel to the beam undeformed axis, the position of a material point is represented by $\mathbf{X}(x) := x\mathbf{e}_1$ where x denotes the coordinate along the straight undeformed beam axis with the origin O fixed at the left end. Therefore, the elastodynamic problem is parameterized with x spanning the compact support $D := \{x | x \in [0,\ell]\}$ – ℓ is the length of the undeformed beam axis – and time t. A material section in the reference configuration is specified by the pair of orthonormal vectors $\mathbf{a}_2$ and $\mathbf{a}_3$, $\mathbf{a}_1 = \mathbf{a}_2 \times \mathbf{a}_3$ so that $\mathbf{a}_i$ is a right-handed orthonormal basis and $\times$ denotes the vector product. Due to body forces $\mathbf{b}(x,t)$ and couples $\mathfrak{m}(x,t)\mathbf{a}_3$ per unit reference length, due to an end load $P(t)\mathbf{e}_1$ applied at the right roller support, the beam is assumed to undergo a naturally planar deformation process in the $(\mathbf{e}_1,\mathbf{e}_2)$-plane, a plane of symmetry for the beam.

Denoting the displacement vector with $\mathbf{u} := u\mathbf{a}_1 + v\mathbf{a}_2$, the current section placement is then defined by $\mathbf{x}(x,t) := \mathbf{X}(x) + \mathbf{u}(x,t)$ and by the pair of orthonormal directors $\mathbf{d}_2(x,t)$ and $\mathbf{d}_3(x,t)$, respectively, with $\mathbf{d}_1 = \mathbf{d}_2 \times \mathbf{d}_3$. The directors $\mathbf{d}_i$ $(i = 1,2)$ can be expressed as $\mathbf{d}_i = \mathbf{R}\mathbf{a}_i$ where $\mathbf{R}(x,t)$ is the proper orthogonal rotation tensor, restricted to the plane $(\mathbf{e}_1,\mathbf{e}_2)$, describing a finite rotation about the $\mathbf{a}_3$-axis.

The beam strains are calculated as the components of the following strain vector and curvature tensor, respectively: $\boldsymbol{\epsilon}(x,t) := \mathbf{R}^\top\mathbf{x}' - \mathbf{X}'$ and $\mathbf{K}(x,t) := \mathbf{R}^\top\mathbf{R}'$ where the prime denotes differentiation with respect to x and $\top$ indicates the transpose.

Because the beam is considered unshearable and inextensible, the internal kinematic constraint $\boldsymbol{\epsilon} = \mathbf{0}$ is enforced thereby leading to

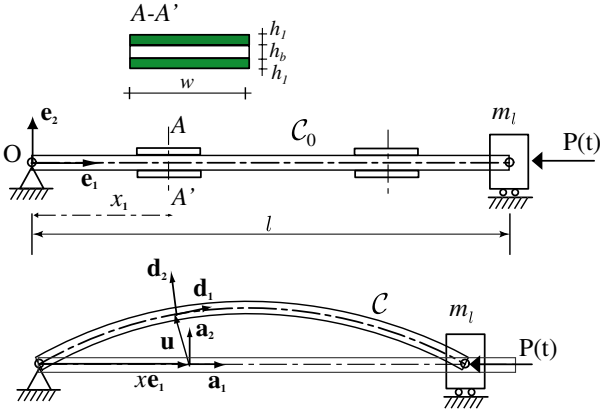

Fig. 1. Scheme of the beam with the end mass in the rest (top) and current (bottom) configurations. A–A' is a cross-section of the piezoceramic patch assembly.

$$\sqrt{(1+u')^2+(v')^2}=1,\quad \theta=\tan^{-1}\left(\frac{v'}{1+u'}\right) \tag{1}$$

Employing $(1)_2$, the bending curvature $k(x,t):=\theta'(x,t)$ is expressed as $k(x,t)=v''+u'v''-u''v'$. Solving the inextensibility constraint, Eq. $(1)_1$ with respect to u' yields $u'=-1\pm\sqrt{1-(v')^2}$ whose expansion in a Mac Laurin series gives, to within second order, $u'\approx-\frac{1}{2}(v')^2$. Consequently, the curvature becomes

$$k(x,t)=\frac{v''}{\sqrt{1-(v')^2}}\approx v''+\frac{1}{2}(v')^2v'' \tag{2}$$

Further, $\sin\theta=v'$ and $\cos\theta=1+u'\approx1-\frac{1}{2}(v')^2$.

Let the internal contact force and couple, mutually exerted by two adjoining sections, be expressed as

$$\mathbf{n}(x,t):=N(x,t)\mathbf{d}_1(x,t)+Q(x,t)\mathbf{d}_2(x,t),\quad \mathbf{m}(x,t):=M(x,t)\mathbf{d}_3 \tag{3}$$

where N and Q indicate the axial load and shear force, respectively, and M is the bending moment. The equilibrium equations, namely the balance of linear momentum and angular momentum, are

$$\mathbf{n}'+\mathbf{b}=\mathbf{0},\quad M'+\mathbf{d}_3\cdot(\mathbf{x}'\times\mathbf{n})+\mathfrak{m}=0 \tag{4}$$

which, once the reactive shear force has been filtered out, are put in componential form

$$\begin{aligned}&N'+kM'+k\mathfrak{m}+b_1=0\\&M''+\mathfrak{m}'-kN-b_2=0\end{aligned} \tag{5}$$

where $\mathbf{b}=b_1\mathbf{d}_1+b_2\mathbf{d}_2$ and the dot indicates the standard inner product in Euclidean space.

Neglecting the rotatory inertia, we express the applied body forces and the translational inertial and distributed damping forces, by virtue of D'Alembert's principle, in the form $\mathbf{b}=\mathbf{f}(x,t)-\rho A\ddot{\mathbf{x}}-(c_u\dot{u}\mathbf{a}_1+c_v\dot{v}\mathbf{a}_2)=(f_1-c_u\dot{u}-\rho A\ddot{u})\mathbf{a}_1+(f_2-c_v\dot{v}-\rho A\ddot{v})\mathbf{a}_2$ where ρ is the beam mass density, A is the area of the cross-section, c_u and c_v denote the viscous damping coefficients in the global longitudinal and transverse directions, respectively, and the overdot indicates differentiation with respect to time. The kinematic boundary conditions are $u(0,t)=0$, $v(0,t)=0$, $v(\ell,t)=0$. Further, the mechanical boundary conditions are

$$M(0,t)=M(\ell,t)=0,\quad N\cos\theta+M'\sin\theta=-m_\ell\ddot{u}-P(t)\quad \text{at } x=\ell \tag{6}$$

where m_ℓ is the lumped mass and $P(t)$ is the end load (see Fig. 1).

From a constitutive point of view, because the curvature is assumed finite but small, a linear constitutive relationship between the bending moment and the curvature is considered in the standard form

$$M(x,t)=E_{\mathrm{b}}I_{\mathrm{b}}(x)k(x,t) \tag{7}$$

where E_{b} and I_{b} indicate Young's modulus and the moment of inertia of the beam cross-section about the $\mathbf{a}_3$-axis, one of the principal inertia axes.

Integrating $(5)_1$ and using the mechanical boundary condition (6) yield the axial load as

$$N(x,t)=-[M'\tan\theta+\sec\theta(m_\ell\ddot{u}+P(t))]|_{x=\ell}-\int_\ell^x kM'\,\mathrm{d}x-\int_\ell^x k\mathfrak{m}\,\mathrm{d}x-\int_\ell^x b_1\,\mathrm{d}x \tag{8}$$

Substituting (8) into $(5)_2$ gives the condensed equation of motion

$$M''+[M'\tan\theta+\sec\theta(m_\ell\ddot{u}+P(t))]|_{x=\ell}k+k\int_\ell^x kM'\,\mathrm{d}x+k\int_\ell^x b_1\,\mathrm{d}x-b_2+\mathfrak{m}'+k\int_\ell^x(k\mathfrak{m})\mathrm{d}x=0 \tag{9}$$

It is worth noting that the bending couples distribution $\mathfrak{m}$ enters the equation of motion (9) as a direct and a non-linear parametric forcing term.

To express the equation of motion in the transverse displacement component only, using the kinematic boundary condition $u(0,t)=0$ and Eq. $(1)_1$, we incorporate the resulting longitudinal motion into the inertial and damping forces, and substitute them along with (2) into (9).

The following non-dimensionalization is suitably employed to render the equations non-dimensional:

$$t^*:=\omega_{\mathrm{b}}t,\quad x^*:=\frac{x}{\ell},\quad v^*:=\frac{v}{l},\quad \alpha:=\frac{m_\ell}{\rho A\ell},\quad P^*:=\frac{\ell^2}{E_{\mathrm{b}}I_{\mathrm{b}}}P,\quad \mathfrak{m}^*:=\frac{\mathfrak{m}\ell^2}{E_{\mathrm{b}}I_{\mathrm{b}}},\quad 2c_v^*:=\frac{c_v\ell^2}{\sqrt{E_{\mathrm{b}}I_{\mathrm{b}}\rho A}} \tag{10}$$

where $\omega_b := [(E_b I_b)/(\rho A \ell^4)]^{1/2}$; the star indicates non-dimensional variables. Henceforth, the star will be dropped for ease of notation and the employed variables will be non-dimensional unless otherwise specified.

The resulting geometrically exact equation of motion is then expanded up to third order thus yielding

$$\ddot{v} + \mathscr{L}v = -2\epsilon^{\nu_1} c_v \dot{v} - \epsilon^{\nu_2} P(t) v'' + \mathscr{N}_3(v,v,v) + \mathscr{I}_3(v,v,\ddot{v}) + \breve{\mathscr{I}}_3(v,\dot{v},\dot{v}) + \mathfrak{m}' + v'' \int_1^x \mathfrak{m} v'' \,\mathrm{d}x \tag{11}$$

where $(\epsilon, \nu_j) \in \mathbb{R}^+, \epsilon \ll 1$ is an ordering parameter, $c_v \in \mathbb{R}^+$ is the distributed beam damping coefficient, $\mathscr{L}v = v''''$ is the linear stiffness term, and the non-linear forces are defined according to the following operators:

$$\mathscr{N}_3(v,v,v) := -[v''' v']|_{x=1} v'' - \left(\frac{1}{2} v'^2 v''\right)'' - v'' \int_1^x v'' v''' \,\mathrm{d}x \tag{12}$$

$$\mathscr{I}_3(v,v,\ddot{v}) := -v' \int_0^x v' \ddot{v}' \,\mathrm{d}x + v'' \int_1^x v' \ddot{v} \,\mathrm{d}x - v'' \int_1^x \int_0^x v' \ddot{v}' \,\mathrm{d}x + \frac{1}{2} \ddot{v} v'^2 + \alpha v'' \int_0^1 v' \ddot{v}' \,\mathrm{d}x \tag{13}$$

$$\breve{\mathscr{I}}_3(v,\dot{v},\dot{v}) := -v' \int_0^x (\dot{v}')^2 \,\mathrm{d}x - v'' \int_1^x \int_0^x \dot{v}'^2 \,\mathrm{d}x + \alpha v'' \int_0^1 \dot{v}'^2 \,\mathrm{d}x \tag{14}$$

The operator $\mathscr{N}_3$ accounts for the internal restoring forces due to the non-linear curvature whereas $\mathscr{I}_3$ and $\breve{\mathscr{I}}_3$ incorporate the non-linear inertia forces ($\mathscr{I}_3$ and $\breve{\mathscr{I}}_3$ are distinctly expressed for computational purposes). The governing mechanical boundary conditions, in their expanded form, are $v'' + \frac{1}{2}(v')^2 v'' = 0$ at both ends.

As to the external bending couples appearing in Eq. (9), these are associated with the control input provided by two piezoceramic actuators, with the kth pair of actuators of length ℓ_k attached to the beam lower and upper surfaces at x_k, the latter being the coordinate of the midspan axis of the piezoceramic patch (Figs. 1, 2, and 4). In the limit case of perfect bonding between the patches and the beam, the mechanical effect of a pair of piezoceramic patches results into two bending couples, of opposite direction exerted at the ends of the patches; hence, the ensuing piezoceramic action in the proposed architecture can be expressed as

$$\mathfrak{m}(x,t) = \sum_{k=1}^{2} \mathscr{M}_k(t)[\delta(x - x_k^-) - \delta(x - x_k^+)] \tag{15}$$

where $\delta(x)$ indicates the Dirac delta function, $x_k^{\mp} := x_k \mp \frac{1}{2}\frac{\ell_k}{\ell}$, and $\mathscr{M}_k(t)$ is the magnitude of the bending moments delivered by the piezoactuators and given, in dimensional form, as

$$\mathscr{M}_k(t) = m_k V_k(t), \quad m_k = \frac{E_b I_b}{2E_b I_b + E_k I_k} E_k (h_b + h_k) w d_{31_k} \tag{16}$$

Here, m_k is the bending couple per unit Volt of the kth pair of patches; $V_k(t)$ is the applied time-varying voltage; w is the common width of the beam and patches; h_k is the thickness of a single patch and I_k is the moment of inertia of a pair of piezoceramic patches with respect to the neutral axis of the assembly; E_k and d_{31_k} are Young's modulus and the transverse charge constant of the kth piezoelectric material, respectively. The non-dimensional couple is $\mathscr{M}_k^* = \mathscr{M}_k \ell^2/(E_b I_b)$.

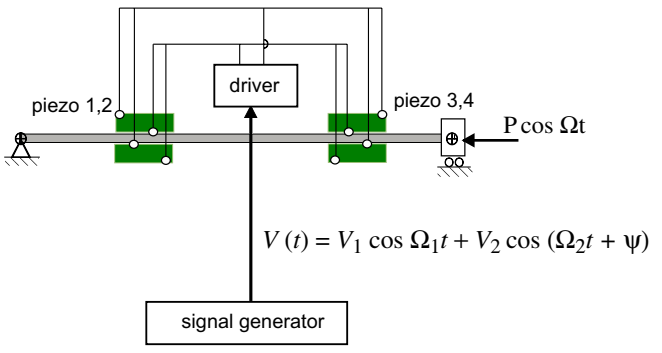

Fig. 2. A schematic view of the beam with the controller scheme.

In conclusion, the control action enters the equations of motion, at leading order, in the non-dimensional form

$$U(x,t) := \mathfrak{m}' = \sum_{k=1}^{2} m_k(t) V_k(t) [H''(x - x_k^-) - H''(x - x_k^+)] \tag{17}$$

where H denotes the Heaviside unit-step function and use of $\delta(x) = H'(x)$ has been made.

3. Design of the control laws via asymptotics

In this section, the resonance cancellation strategy, devised employing a perturbation approach, is illustrated. The method of multiple scales is used to attack directly the governing equation of motion and boundary conditions instead of treating finite-degree-of-freedom discretized versions. With this approach, the problem of order reduction is overcome along with other drawbacks such as spillover effects potentially arising from the unmodelled dynamics.

The disturbance is caused by a harmonic end load, $P(t) := P\cos\Omega t$ with $\Omega \approx 2\omega_2$, where ω_2 is the circular frequency of the second mode. To design the control laws, we determine the responses of the beam to a principal parametric resonance of the second mode when this mode is away from internal resonances, that is, it can not interact with any other mode.

The objective of the sought control algorithm is to activate – applying symmetric control actions – internal forces possessing skew-symmetric components and of a like type as those induced by the external principal parametric resonance, that is, $\propto \overline{A}\exp(\mathrm{i}\omega_2 t)$ where i is the imaginary unit and A indicates the complex-valued amplitude of the response at the system second natural frequency and the bar denotes the complex conjugate. Guided by the fact that the non-linear forces are cubic, the control signal (i.e., the applied voltage) is assumed as a two-frequency input in the form

$$V(t) = \frac{1}{2}\left[V_1 \mathrm{e}^{\mathrm{i}\Omega_1 t} + V_2 \mathrm{e}^{\mathrm{i}(\Omega_2 t + \psi)}\right] + \mathrm{cc} \tag{18}$$

where cc indicates the complex conjugate of the preceding terms and ψ is the relative phase between the control signals. A symmetric controller arrangement is obtained (see Fig. 2) by two pairs of like-length piezoceramic patches ($\ell_1 = \ell_2$) with $x_1 + x_2 = 1$ and $m_1 = m_2 = m_p$. Consequently, the control action takes the form

$$U(x,t) = \frac{1}{2} m_p [V_1 \mathrm{e}^{\mathrm{i}\Omega_1 t} + V_2 \mathrm{e}^{\mathrm{i}(\Omega_2 t + \psi)}] \sum_{k=1}^{2} [H''(x - x_k^-) - H''(x - x_k^+)] + \mathrm{cc} \tag{19}$$

The two control frequencies are chosen so as to activate a sub-combination resonance of the sum or difference type with the excited mode. The resulting response at leading order is $\propto [A\exp(\mathrm{i}\omega_2 t), V_1\exp(\mathrm{i}\Omega_1 t), V_2\exp(\mathrm{i}\Omega_2 t)]$. Therefore, part of the induced third-order non-linear forces are $\propto m_p^2 V_1 V_2 \overline{A}\exp(\mathrm{i}\omega_2 t)$ if and only if

$$\frac{\Omega_2 \pm \Omega_1}{2} \approx \omega_2 \tag{20}$$

This equation expresses the condition on the effective control frequencies.

3.1. Asymptotic analysis

A third-order uniform expansion of the solutions of the equation of motion is determined letting the deflection v and associated velocity field $\dot{v}$ be in the form

$$\begin{aligned} v(x,t) &= \epsilon v_1(x,t_0,t_2) + \epsilon^3 v_3(x,t_0,t_2) + \mathrm{O}(\epsilon^5) \\ \dot{v}(x,t) &= \epsilon \dot{v}_1(x,t_0,t_2) + \epsilon^3 \dot{v}_3(x,t_0,t_2) + \mathrm{O}(\epsilon^5) \end{aligned} \tag{21}$$

where $t_0 = t$ is the fast scale associated with variations occurring at the frequency of the second mode, and $t_2 = \epsilon^2 t$ is the stretched time scale governing the non-linear slow variations. The small dimensionless parameter

ϵ is the same parameter introduced in the non-dimensional equation of motion as ordering device. Consequently, the first derivative with respect to time is $\frac{\partial}{\partial t} = D_0 + \epsilon^2 D_2 + \mathrm{O}(\epsilon^4)$ where $D_n := \frac{\partial}{\partial t_n}$. Further, the nearness of the principal parametric resonance is expressed introducing a detuning parameter σ_1 such that $\Omega = 2\omega_2 + \epsilon^2 \sigma_1$, whereas the detuning condition of the sub-combination resonance is $\Omega_2 \pm \Omega_1 = 2\omega_2 + \epsilon^2\sigma_2$ with $(\sigma_1, \sigma_2) = \mathrm{O}(1)$.

The external excitation and damping are ordered by letting $v_1 = v_2 = 2$ so that the damping, excitation and non-linear resonant forces balance each other at third order. Substituting (21) into the system of first-order (in time) equations of motion and boundary conditions, using the independence of the time scales, and equating coefficients of like powers of ϵ yields

Order ϵ

$$\begin{aligned} &D_0 v_1 - \dot{v}_1 = 0 \\ &D_0 \dot{v}_1 + \mathscr{L} v_1 = \frac{1}{2} m_p [V_1 \mathrm{e}^{\mathrm{i}\Omega_1 t_0} + V_2 \mathrm{e}^{\mathrm{i}(\Omega_2 t_0 + \psi)}] \sum_{k=1}^{2} [H''(x - x_k^-) - H''(x - x_k^+)] + \mathrm{cc} \end{aligned} \tag{22}$$

Order ϵ^3

$$\begin{aligned} &D_0 v_3 - \dot{v}_3 = -D_2 v_1 \\ &D_0 \dot{v}_3 + \mathscr{L} v_3 = -D_2 \dot{v}_1 - 2c_v D_0 \dot{v}_1 + \mathscr{N}_3(v_1, v_1, v_1) + \mathscr{I}_3(v_1, v_1, D_0 \dot{v}_1) + \breve{\mathscr{I}}_3(v_1, \dot{v}_1, \dot{v}_1) \\ &\qquad + v_1'' \int_1^x \mathrm{m} v_1'' \,\mathrm{d}x - \left(\frac{P}{2} \mathrm{e}^{\mathrm{i}\Omega t_0} v_1'' + \mathrm{cc} \right) \end{aligned} \tag{23}$$

For a simply supported beam, the natural frequencies and associated eigenfunctions are $\omega_n = n^2\pi^2$ and $\phi_n(x) = \sqrt{2}\sin n\pi x, n = 1, 2, \ldots$ The latter are normalized in the standard fashion, $\int_0^1 \phi_m \phi_n \,\mathrm{d}x = \delta_{mn}$, $\int_0^1 \phi_m \mathscr{L} \phi_n \,\mathrm{d}x = \omega_n^2 \delta_{mn}$ where δ_{mn} is the Kronecker delta.

Because the second mode is directly excited by the parametric resonance disturbance and, indirectly, by the control input and because this mode is away from internal resonances, the solution at order ϵ is assumed as

$$v_1 = \frac{1}{2} m_p \sum_{j=1}^{2} [V_j \mathrm{e}^{\mathrm{i}(\Omega_j t_0 + \psi_j)} \mathscr{B}_j(x)] + A(t_2) \mathrm{e}^{\mathrm{i}\omega_2 t_0} \phi_2(x) + \mathrm{cc} \tag{24}$$

where $\psi_1 = 0$, $\psi_2 = \psi$, and the functions $\mathscr{B}_j(x)$ are solutions of the following boundary-value problems:

$$\mathscr{B}_j'''' - \Omega_j^2 \mathscr{B}_j = \sum_{k=1}^{2} [H''(x - x_k^-) - H''(x - x_k^+)] \tag{25}$$

with the boundary conditions $\mathscr{B}_j(0) = \mathscr{B}_j(1) = 0$ and $\mathscr{B}_j''(0) = \mathscr{B}_j''(1) = 0$, $j = 1, 2$.

The solutions of these two boundary-value problems are obtained, using the modal expansion method, as infinite series of the symmetric eigenmodes in the form

$$\mathscr{B}_j(x) = \sum_{k=0}^{\infty} \frac{b_{2k+1}}{\omega_{2k+1}^2 - \Omega_j^2} \phi_{2k+1}(x) \tag{26}$$

where

$$b_j := \phi_j'(x_1^+) - \phi_j'(x_1^-) + \phi_j'(x_2^+) - \phi_j'(x_2^-) \tag{27}$$

is the jth modal force produced by unitary moments delivered by the two pairs of actuators. Substituting the first-order solution into the third-order problem, and enforcing the solvability of the resulting inhomogeneous partial-differential problem yields the following modulation equation:

$$2\mathrm{i}\omega_2(\dot{A} + \mu A) = \mathbb{G} A^2 \overline{A} + \mathbb{U}_s A + P\mathbb{K}\overline{A}\mathrm{e}^{\mathrm{i}\sigma_1 t} + \mathbb{U}\overline{A}\mathrm{e}^{\mathrm{i}(\sigma_2 t + \psi)} \tag{28}$$

where $\mu := c_v$ is the beam damping coefficient (the damping ratio of the second mode is $\zeta = \mu/\omega_2$); $\mathbb{G}$ and $\mathbb{K}$ are the *effective non-linearity coefficient* and the *effective parametric resonance coefficient*, respectively, given by

$$\mathbb{G} := \pi^4(17098.2 - 288\pi^2) + (49873.4\pi^4)\alpha, \quad \mathbb{K} := -\frac{1}{2}\int_0^1 (\phi_2 \phi_2'')\mathrm{d}x = 2\pi^2 \tag{29}$$

On the other hand, $\mathbb{U}$ and $\mathbb{U}_s$ are the *effective control coefficient* and the linear *frequency shift coefficient*, respectively, expressed as

$$\mathbb{U} = m_p^2 V_1 V_2 B_3, \quad \mathbb{U}_s = B_1 V_1^2 + B_2 V_2^2 \tag{30}$$

The coefficients B_1, B_2, and B_3 are obtained as outcome of the solvability condition. The coefficient B_3 can be conveniently expressed as $B_3 = B_3^0 + B_3'\alpha$ so as to outline the influence of the boundary mass ratio α on the effective control coefficient.

In the next section, the remaining control parameters, namely, the phase and gains, are determined. To this end, we first transform the complex-valued modulation equation into real-valued equations governing the amplitude and phase of the motion. We assume a polar transformation of the complex-valued amplitude in the form $A = \frac{1}{2} a e^{i(\sigma_1 - \gamma)\frac{t}{2}}$.

The structure of the modulation equation suggests that it can be rendered autonomous if the control frequency detunings satisfy the condition $\sigma_2 = \sigma_1 =: \sigma$. The control frequencies can then be more conveniently expressed as $\Omega_1 = \frac{m_1}{n_1}\Omega$ and $\Omega_2 = \frac{m_2}{n_2}\Omega$ with

$$\frac{m_2}{n_2} \pm \frac{m_1}{n_1} = 1 \tag{31}$$

The resulting frequency–response equation for the steady-state responses is

$$\sigma = -\left(\frac{\mathbb{U}_s}{\omega_2} + \frac{\mathbb{G}}{4\omega_2} a^2\right) \pm \sqrt{\frac{\mathbb{F}^2}{\omega_2^2} - 4\mu^2} \tag{32}$$

where $\mathbb{F} := P\mathbb{K} \pm \mathbb{U}$, the sign $\pm$ depends on whether $\psi = 0$ or π as it will be shown. The solution for the uncontrolled case can be obtained from (32) setting $V_1 = V_2 = 0$. The parametric resonance, in the absence of controls, is activated when the end load P is larger than the threshold value given by $P_{cr} = 2\omega_2 \frac{\mu}{\mathbb{K}}$. The uncontrolled deflection, to within first order, can be expressed as

$$v(x,t) \approx a \cos\left[\frac{1}{2}(\Omega t - \gamma)\right] \phi_2(x) \tag{33}$$

3.2. Design of the control phase and gains

We require the control-induced force to be in the opposite complex direction of the external parametric-resonance force; on account of the fact that $\mathbb{K} > 0$, the relative control phase is determined as

$$\psi = 0, \quad \text{if } \mathbb{U} < 0 \quad \text{and} \quad \psi = \pi, \quad \text{if } \mathbb{U} > 0 \tag{34}$$

Since the threshold for the activation of the parametric resonance is $|\mathbb{F}| = 2\mu\omega_2$, to inhibit the resonance, we determine $\mathbb{U}$ such that $|\mathbb{F}| < 2\mu\omega_2$. Accounting for the phase information, $\mathbb{F} = P\mathbb{K} - |\mathbb{U}|$, then the inequality entails that the combined control gains, $V_c := V_1 V_2$, must satisfy the following inequality:

$$V_{c1} \leqslant V_c \leqslant V_{c2}, \quad \text{with } V_{c1,2} = \frac{P\mathbb{K} \mp 2\mu\omega_2}{m_p^2 |B_3|} \tag{35}$$

Selecting (V_1, V_2) such that V_c is within the range given by (35), the parametric resonance is annihilated and the steady-state controlled transverse displacement field, to within first order, can be expressed as

$$v(x,t) \approx m_p \left[V_1 \mathscr{B}_1(x) \cos\left(\frac{m_1}{n_1}\Omega t\right) + V_2 \mathscr{B}_2(x) \cos\left(\frac{m_2}{n_2}\Omega t + \psi\right)\right] \tag{36}$$

To find the optimal gains (V_1, V_2) within the bounds (35), we choose to minimize, over one period of oscillation, the maximum amplitude of the integral of the square of the deflection at steady state, namely,

$$J = \int_0^1 v(x,t)^2 \, \mathrm{d}x = m_p^2 [J_1 V_1^2 \cos^2 \Omega_1 t + J_2 V_2^2 \cos^2(\Omega_2 t + \psi) + 2 J_3 V_1 V_2 \cos \Omega_1 t \cos(\Omega_2 t + \psi)] \tag{37}$$

where

$$J_{1,2} = \sum_{k=0}^{\infty} \frac{b_{2k+1}^2}{\left(\omega_{2k+1}^2 - \Omega_{1,2}^2\right)^2}, \quad J_3 = \sum_{k=0}^{\infty} \frac{b_{2k+1}^2}{(\omega_{2k+1}^2 - \Omega_1^2)(\omega_{2k+1}^2 - \Omega_2^2)} \tag{38}$$

3.3. Different sub-combination resonance control laws

We have investigated two control laws based on sub-combination resonances of the difference type, $\Omega_2 - \Omega_1 \approx 2\omega_2$. In particular, the considered control laws are

$$\begin{aligned} &\text{I}: \left(\frac{m_1}{n_1} = 1, \frac{m_2}{n_2} = 2\right) \quad (\Omega_1 = \Omega, \Omega_2 = 2\Omega) \\ &\text{II}: \left(\frac{m_1}{n_1} = \frac{3}{4}, \frac{m_2}{n_2} = \frac{7}{4}\right) \quad \left(\Omega_1 = \frac{3}{4}\Omega, \Omega_2 = \frac{7}{4}\Omega\right) \end{aligned} \tag{39}$$

More elaborate control laws based on simultaneous resonances may be further devised. For example, the condition $\Omega_1 \approx 3\omega_2$ and $\Omega_2 \approx 5\omega_2$ entails the presence of two simultaneous resonances, namely a sub-harmonic resonance of order one-third ($\Omega_1 \approx 3\omega_2$) and a sub-combination resonance of the difference type. However, this control law is not here investigated.

4. Results and discussion

The test specimen employed in the experimental investigations is a uniform beam with a rectangular cross-section made of phosphore bronze and two pairs of piezoceramic patches (FUJI CERAMICS Corporation, Z0.3T10x45R-SYX) attached at one- and three-quarters of the beam span. The main properties of the beam and of the piezoactuators are summarized in Table 1. The apparatus (Fig. 3) consists of the test specimen with its hinges made of radial bearings (JIS 6200). The width direction has been placed in a vertical plane to overcome the presence of initial curvature due to gravity. The radial bearings are accurately manufactured and have been cleaned using a procedure consisting in injecting a special high-lubrication oil with high-pressure (Kure 556). One of the hinges is rigidly clamped onto an aluminum slab. The other hinge is mounted on top of a sliding linear bearing (IKO Ball Slide Unit, Model BSU 44-50 A). On the lateral end of the linear bearing (Fig. 3), a linear motor (Showa-Densen-Denran Model 26-02R) applies the dynamic axial force. A TOA Electronics waveform synthesizer model FS-2201 feeds the sinusoidal signal to a KIKUSUI power amplifier model BIPOLAR PBX40-10 which, in turn, drives the linear motor. A KEYENCE LB-01 (resolution of 180 μm and sampling time of 0.7 ms) laser sensor was used to measure the displacement of the beam at one-quarter of the beam span.

First, we experimentally characterized the principal parametric resonance of the second mode and compared the experimental results with the theoretical predictions. Subsequently, we investigated the effectiveness of the resonance-cancellation scheme. In the next section, the parametric resonance without controls is discussed.

Table 1
Properties of the tested beam and piezoceramic patch

	Beam	PZT
Length (mm)	450	45
Width (mm)	10	10
Thickness (mm)	0.5	0.3
Density (kg/m^3)	9.2×10^3	7.65×10^3
Young's modulus (GPa)	116	62
Piezoelectric constant (m/V)	–	-2.1×10^{-10}

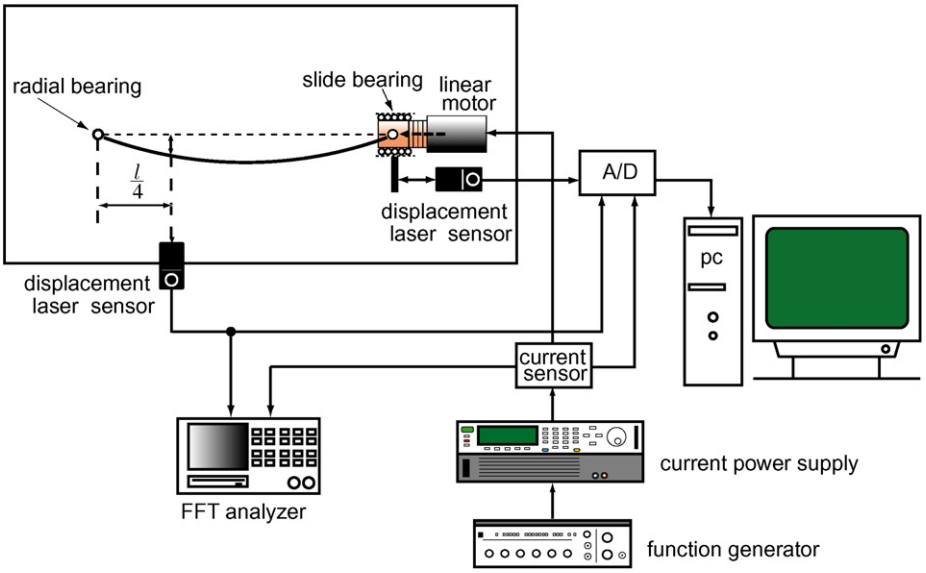

Fig. 3. Schematic view of the experimental setup.

4.1. Parametric resonance of the second mode

We first tested the piezoceramic patches measuring the static beam response to a constant voltage input, $V = 150$ V, with a two-fold objective: to identify the properties of the actuators and confirm the level of fidelity of the model of the piezoceramic action used in the analysis. In Fig. 4, we show the theoretically obtained beam deflection under the applied DC voltage and the distribution of the bending moment, obtained from (26), putting $\Omega_j = 0$, and (7), respectively. In dimensional form,

$$v(x) = V\left(\frac{m_p \ell^3}{E_b I_b}\right) \sum_{k=0}^{\infty} \frac{b_{2k+1}}{\omega_{2k+1}^2} \phi_{2k+1}(x), \quad M(x) = V(m_p \ell) \sum_{k=0}^{\infty} \frac{b_{2k+1}}{\omega_{2k+1}^2} \phi''_{2k+1}(x) \tag{40}$$

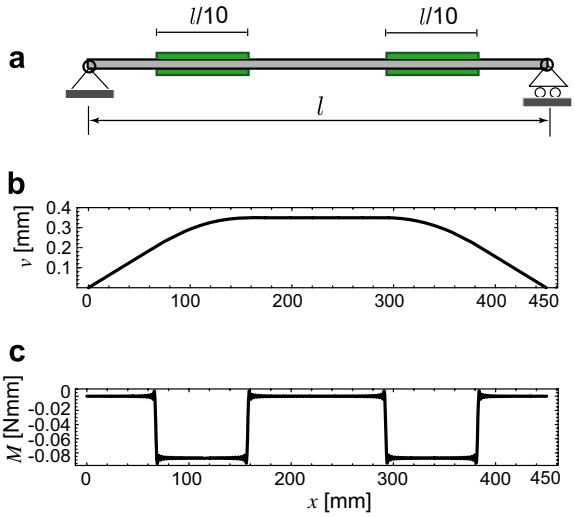

Fig. 4. (a) Scheme of the beam with the experimental piezoceramic patch assembly, (b) beam static deflection, and (c) static bending moment when $V = 150$ V.

We observe that, using the modal expansion of the static solution, the displacement is well described by five functions whereas a higher number of functions, at least 10 times, is required to reproduce the piece-wise constant character of the bending moment. At one-quarter of the beam span, the laser sensor detected a displacement of 0.28 mm whereas the theoretical prediction, according to the parameters given in Table 1, is 0.34 mm.

Then, the natural frequency of the second mode was measured and turned out to be 15.1 Hz which is in close agreement with the theoretical prediction of 15.38 Hz. To characterize the resonance, in Fig. 5, we show the theoretically obtained and experimentally detected parametric resonance unstable region (also known as *Mathieu tongue*), in the plane of the force frequency and amplitude. The experimental procedure consisted in determining the tip of the tongue fixing the frequency at twice the natural frequency of the second mode and increasing the end load amplitude from a low value until activating the resonance at its threshold value. Then, the amplitude of the force was increased and a frequency sweep was performed. The resonance tongue denoted with a solid line was computed using the presented theory. The agreement between the theory and the experiments is good both qualitatively and quantitatively.

Moreover, to confirm the non-linear characteristic of the mode and the dependence of the width of the unstable region on the forcing amplitude, we measured some frequency–response curves. In Fig. 6, we show the theoretically and experimentally obtained frequency–response curves when the force is nearly twice the threshold force, namely, $P = 0.64$ N. The first skew-symmetric mode is clearly a softening mode. Considering

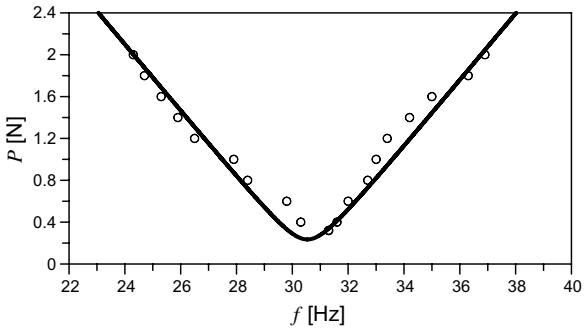

Fig. 5. Experimentally (dots) and theoretically (solid line) obtained parametric resonance region in the plane of the disturbance frequency (in Hz) and amplitude (in N) when the modal damping ratio is $\zeta = 0.05$.

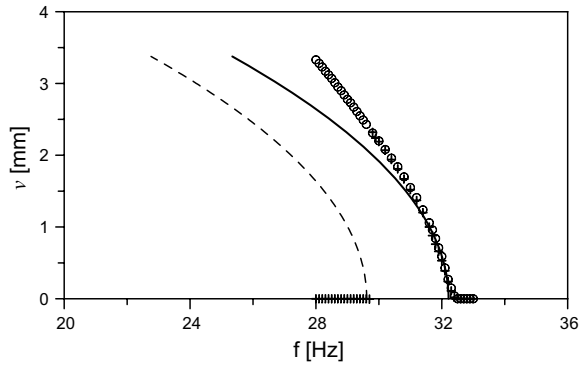

Fig. 6. Experimentally and theoretically obtained frequency–response curve of the principal parametric resonance of the second mode when $P = 0.64$ N and the modal damping ratio is $\zeta = 0.05$. The dots (crosses) indicate backward (forward) frequency sweeps. The solid (dashed) line denotes analytical stable (unstable) solutions.

the end mass ratio $\alpha = 9.8$, the calculated effective non-linearity coefficient is $\mathbb{G} = 4.5 \times 10^7$. Because $\mathbb{G} > 0$, the mode is predicted as softening. Moreover, the trivial solution exhibits a supercritical pitchfork bifurcation around 32.1 Hz and a subcritical pitchfork bifurcation around 29.8 Hz. The maximum amplitude is of the order of 3 mm. The agreement is good at low amplitudes as expected. At higher amplitudes, a higher-order expansion of the resonance seems to be necessary to capture more accurately the behaviour. In the next section, we discuss the main theoretical results relating to the resonance-cancellation scheme and the experimental validation.

4.2. Resonance-cancellation: theoretical and experimental results

The feasibility and effectiveness of the resonance-cancellation laws were theoretically investigated so as to determine also the suitable ranges of the gains before performing the experiments. First, we computed the second-order shape functions shown in Fig. 7 according to the control laws I and II. Generally, five terms only in the series were sufficient for convergence. Performing the calculations, the results for the coefficients B_1, B_2, and B_3 of the control laws are summarized in Table 2. The control laws I and II require a relative phase $\psi = 0$.

In Fig. 8, we show variation of the ranges of the effective control gains with the load amplitude according to the control laws I and II. Considering the combined voltage gain, $V_c = V_1 V_2$, the regions of effective gains are bounded by straight and parallel lines given by $V_{c1,2}$. However, assuming the same gains for both signals (i.e, $V_1 = V_2$), then, the regions are bounded by non-linear curves. Clearly, these curves are meaningful only when $P > P_{cr}$. There is a rapid increase of the required voltage right above the instability, thereafter the increase rate

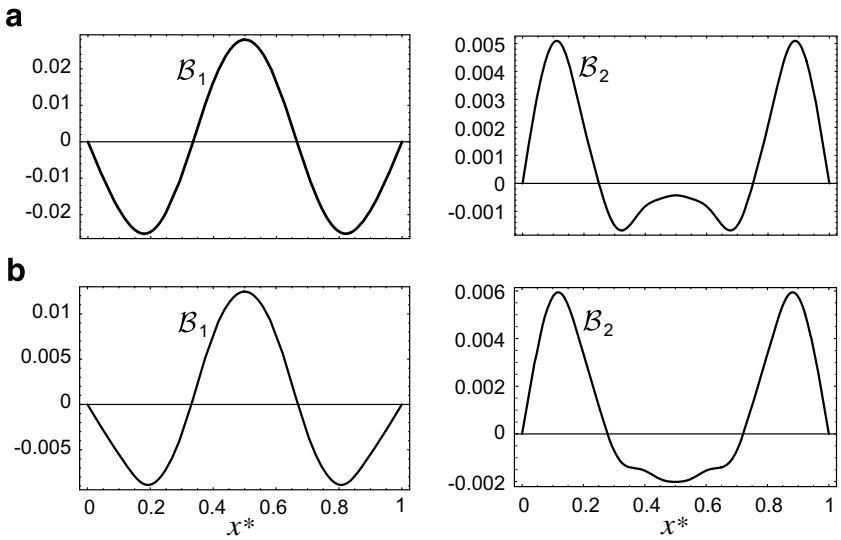

Fig. 7. The functions $\mathscr{B}_1(x)$ (left) and $\mathscr{B}_2(x)$ (right) associated with the response to the control inputs with frequencies Ω_1 and Ω_2, respectively, and according to the control laws I (a) and II (b).

Table 2
Control law coefficients

Control law	B_1	B_2	B_3^0	B_3'
I	294.841	−15.678	−22.183	−146.203
II	55.339	−15.795	−27.273	−75.198

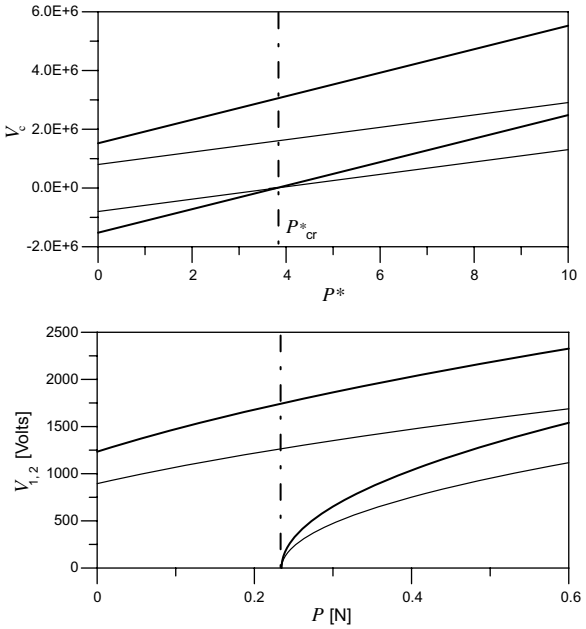

Fig. 8. Regions of the effective control gains according to the control laws I (thick line) and II (thin line), respectively.

flattens out. After calculating the optimal gains within these regions, we obtained the non-dimensional time histories of the one-quarter span section and compared the uncontrolled deflection with the controlled beam deflection when $\sigma = -25$ (Fig. 9). We observe that, for optimal gains, besides suppressing the parametric resonance, a reasonable reduction of the vibration amplitude may also be achieved. Mention must be made of the fact that, as expected, the resulting reduced steady-state vibrations are symmetric.

Next, we show the main experimental results. In Fig. 10(a) and (b), we show the time history and FFT of the excitation force whose amplitude is $P = 0.42$ N and the frequency is $\Omega = 32$ Hz. In Fig. 10(c) and (d), the time history and FFT of the beam response are shown. The activation of the parametric resonance is testified by the high peak at the beam non-linear natural frequency, namely $\Omega/2$. Thereafter, we tested the control law I considering suitable control inputs; the associated time history and FFT are shown in Fig. 11(c) and (d). The resulting beam response to the control force, shown in Fig. 11(a) and (b), is reported in Fig. 11(e) and (f). In the FFT of the response, besides the main predicted peak at the control signal frequency Ω and a minor peak at 2Ω, we note that the second mode frequency is cancelled. An overall vibration reduction of the order of 25% is attained. Since the primary control objective of the methodology is fulfilled cancelling the parametric resonance of a skew-symmetric mode using a non-collocated input, the reduction of the resulting overall response is a secondary task. Fine tuning of the control gains to the optimal values can lead to an enhanced reduction although this has not been pursued.

Moreover, to investigate the capability of the control system of performing while the resonance is fully developed, we let the beam attain the parametric-resonance steady-state and then turned on the controller. The recorded input and response are shown in Fig. 12(a) and (b). In the beam response (Fig. 12a), according to the FFT analyzer, the second mode does not contribute to the beam response. Further, the recovery of the parametric resonance activation, in the absence of controls, is shown in Fig. 12(d) where the controller was turned off at a certain time as clear in Fig. 12(c).

In previous studies, although relating to different systems – a shallow arch in Lacarbonara et al. (2002) and a magnetically levitated body in Yabuno et al. (2004b) – the sensitivity of the controller was investigated against perturbations, consisting of a series of additional impulses or detunings in the excitation amplitude and frequency. It was therein shown that the control was still effective in maintaining its control performance, that is, the suppression of the parametric resonance.

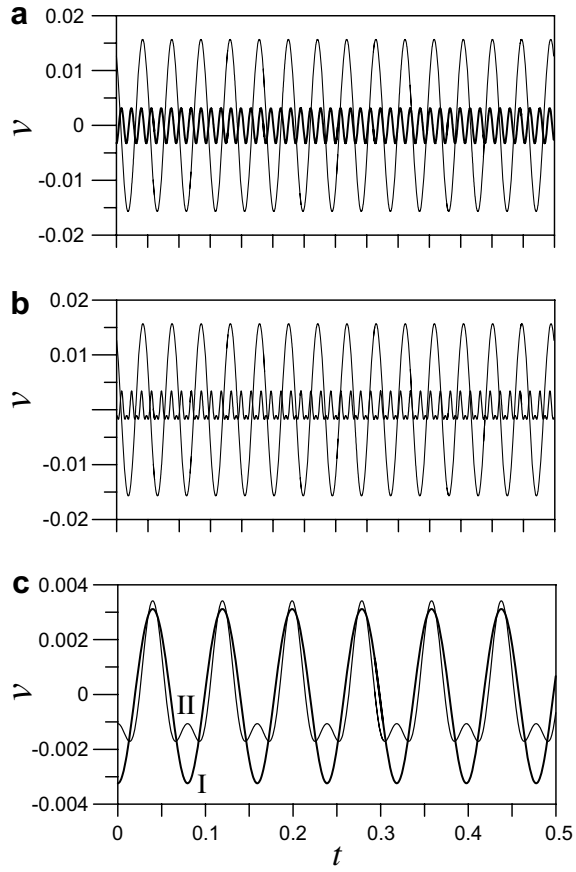

Fig. 9. The steady-state deflections at one-quarter span of the uncontrolled (thin line) and controlled (thick line) beam when $P^* = 9.65$ and $\sigma = -25$ according to (a) the control law I (thick line) and (b) control law II (thin line), respectively. In part (c), the controlled responses are superimposed.

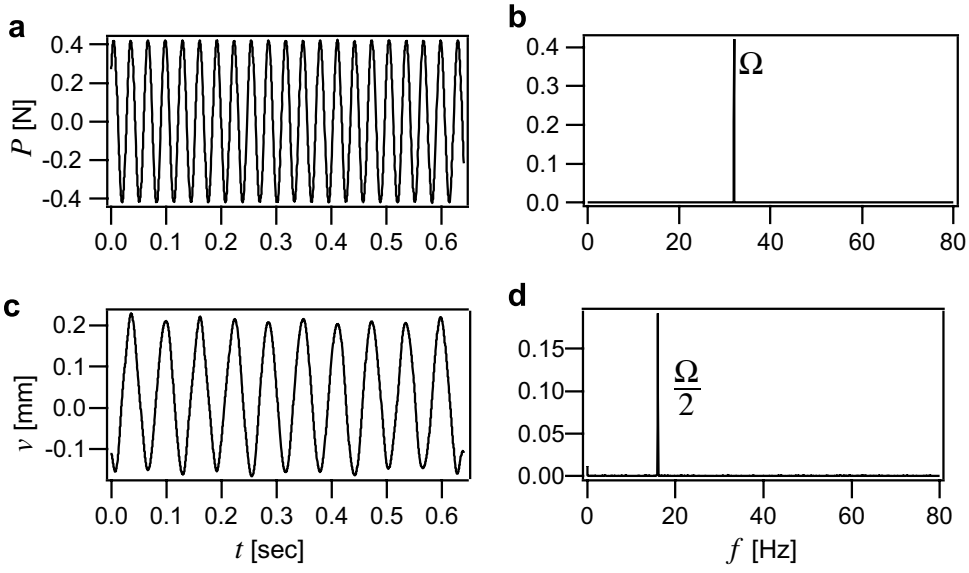

Fig. 10. (a) Time history and (b) FFT of the excitation force when $P = 0.42$ N; (c) time history and (d) FFT of the uncontrolled beam response at $x = \ell/4$.

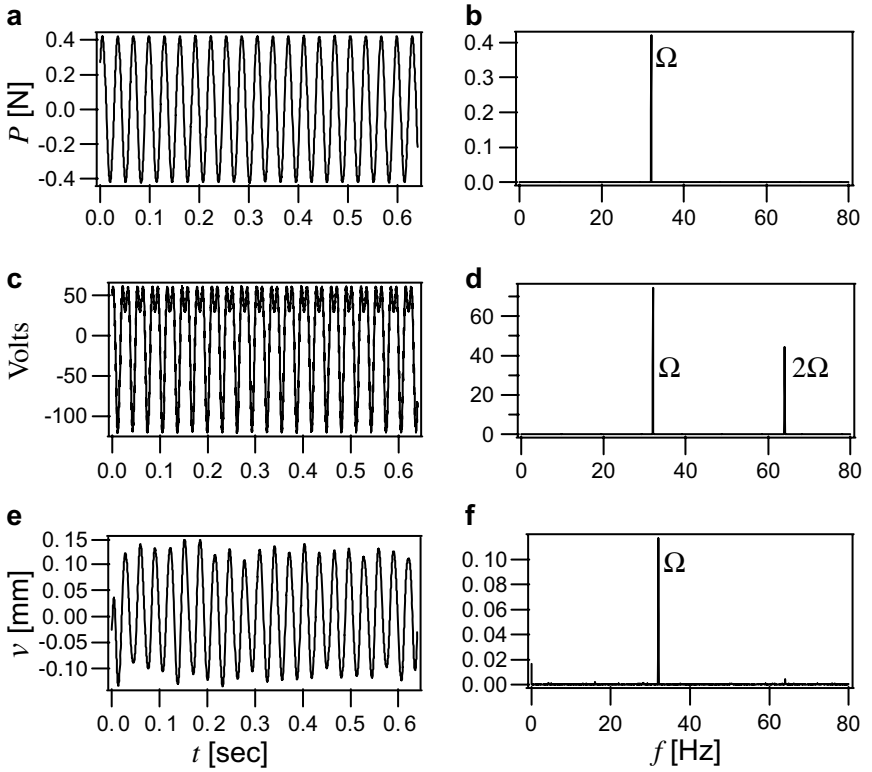

Fig. 11. (a) Time history and (b) FFT of the input force; (c) time history and (d) FFT of the control signal (volts) according to the control law I; (e) time history and (f) FFT of the controlled beam response at $x = \ell/4$ when $P = 0.42$ N.

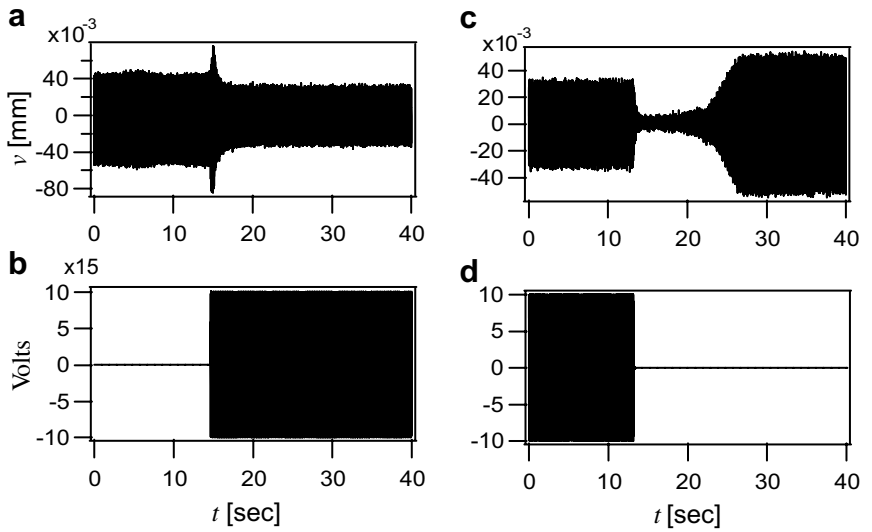

Fig. 12. (a) Time history of the control input and (b) the corresponding beam response when $P = 0.36$ N; (c) time history of the control input and (d) the corresponding beam response.

5. Concluding remarks

In this work the effectiveness of a non-linear strategy for cancelling the parametrically forced skew-symmetric vibrations of a straight elastic beam via a non-collocated input has been theoretically and experimentally

investigated. The control strategy inhibits activation of the principal parametric resonance of the lowest skew-symmetric mode using two pairs of symmetrically located piezoceramic actuators. The control algorithm is open loop because state variables are not used for feedback. The difficulty arises because the disturbance input and actuator are not physically collocated and the control action is linearly orthogonal to the excited mode. The key idea is to rely on part of the suitably determined non-linear controller action which is not orthogonal to the mode and further possesses stabilization effects.

We show that a perturbation analysis can be used to design the proper form of the control input. A control law based on a two-frequency signal, which is involved in a sub-combination resonance (of the difference or additive type) with the excited mode, is used for suppressing the parametric resonance. The control signals are selected as proper ultra-sub-harmonics of the external excitation frequency and, hence, are phase-locked with the disturbance. The control action is effective in cancelling the resonance provided that the gains are within certain theoretically determined bounds. These bounds allow for sufficient control gain detunings and, further, allow optimal reduction of the residual vibrations at the frequencies of the control inputs.

The theoretical predictions have been validated by the experimental results relating both to the uncontrolled parametric resonance of the second mode of a simply supported beam and to the control strategy. The employed equations of motion including the piezoceramic actuators predict the beam responses with high fidelity. In particular, the static response of the beam to a DC piezoactuation has first been validated. Then, the resonance instability region of the second mode and frequency–response curves have been measured to validate the model. The control signal involving a sub-combination resonance of the difference type has been experimentally proved to be capable of achieving resonance cancellation. An overall optimization of the control scheme can be further pursued. The main contribution, however, is the demonstration that, contrary to non-collocated linear control schemes, a relatively simple open-loop control system, relying on non-linear phenomena, is effective in cancelling both symmetric and skew symmetric parametric resonances.

Acknowledgements

This work was partially supported by the Japanese Ministry of Education, Culture, Sports, Science and Technology, under Grants-in-Aid for Scientific Research 16560377 and by the Italian Ministry of Education, University and Scientific Research under the FY 2003–2004 PRIN Grant "Analysis, experiment, identification, control of models, prototypes and full-scale structures".

References

Fujino, Y., Warnitchai, P., Pacheco, B.M., 1993. Active stiffness control of cable vibration. Journal of Applied Mechanics 60, 948–953.

Ji, J.C., Leung, A.Y.T., 2002. Bifurcation control of a parametrically excited Duffing system. Nonlinear Dynamics 27, 411–417.

Lacarbonara, W., Yabuno, H., 2004. Closed-loop non-linear control of an initially imperfect beam with non-collocated input. Journal of Sound and Vibration 273, 695–711.

Lacarbonara, W., Yabuno, H., 2006. Refined models of elastic beams undergoing large in-plane motions: theory and experiment. International Journal of Solids and Structures 43, 5066–5084.

Lacarbonara, W., Chin, C.-M., Soper, R.R., 2002. Open-loop non-linear vibration control of shallow arches via perturbation approach. Journal of Applied Mechanics 69, 325–334.

Maccari, A., 2001. The response of a parametrically excited van der Pol oscillator to a time delay state feedback. Nonlinear Dynamics 26 (2), 105–119.

Oueini, S.S., Nayfeh, A.H., 1999. Single-mode control of a cantilever beam under principal parametric excitation. Journal of Sound and Vibration 224 (1), 33–47.

Oueini, S.S., Nayfeh, A.H., Pratt, J.R., 1998. A non-linear vibration absorber for flexible structures. Nonlinear Dynamics 15, 259–282.

Soper, R.R., Lacarbonara, W., Nayfeh, A.H., Mook, D.T., 2001. Open-loop resonance-cancellation control for a base-excited pendulum. Journal of Vibration and Control 7, 1265–1279.

Watanabe, T., Ohishi, J., Yasuda, K., 2003. Robust damping control of power oscillation incorporating parametric resonance. Electrical Engineering in Japan 142 (1), 42–49.

Yabuno, H., Murakami, T., Kawazoe, J., Aoshima, N., 2004a. Suppression of parametric resonance with a pendulum. Journal of Vibration and Acoustics 126, 149–162.

Yabuno, H., Kanda, R., Lacarbonara, W., Aoshima, N., 2004b. Non-linear active cancellation of the parametric resonance in a magnetically levitated body. Journal of Dynamic Systems, Measurement and Control 126, 433–442.